(4)

OFFICE OF NAVAL RESEARCH

Contract N00014-80-K-0852

R&T Code_____

Technical Report No. 47

Utilization of a Highly Correlated Cluster Model for Interpretation of Electronic Spectroscopic Data for The High-Temperature Superconductors

By

D. E. Ramaker

Prepared for Publication

in the

AIP/AVS Topical Conference Proceedings

George Washington University
Department of Chemistry
Washington, D.C. 20052

December, 1988

ADA202080

SECURITY CLASSIFICATION OF THIS PAGE

REPORT DOCUMENTATION PAGE

1a. REPORT SECURITY CLASSIFICATION Unclassified	1b. RESTRICTIVE MARKINGS
2a. SECURITY CLASSIFICATION AUTHORITY	3. DISTRIBUTION / AVAILABILITY OF REPORT Approved for Public Release, distribution Unlimited.
2b. DECLASSIFICATION / DOWNGRADING SCHEDULE	
4. PERFORMING ORGANIZATION REPORT NUMBER(S) Technical Report # 47	5. MONITORING ORGANIZATION REPORT NUMBER(S)
6a. NAME OF PERFORMING ORGANIZATION Dept. of Chemistry George Washington Univ.	6b. OFFICE SYMBOL (If applicable)
6c. ADDRESS (City, State, and ZIP Code) Washington, D.C. 20052	7a. NAME OF MONITORING ORGANIZATION Office of Naval Research (Code 413)
	7b. ADDRESS (City, State, and ZIP Code) Chemistry Program 800 N. Quincy Street Arlington, VA 22217
8a. NAME OF FUNDING / SPONSORING ORGANIZATION Office of Naval Research	8b. OFFICE SYMBOL (If applicable)
	9. PROCUREMENT INSTRUMENT IDENTIFICATION NUMBER Contract N00014-80-K-0852
8c. ADDRESS (City, State, and ZIP Code) Chemistry Program 800 North QUINCY, Arlington, VA 22217	10. SOURCE OF FUNDING NUMBERS PROGRAM ELEMENT NO. 61153 N; PROJECT NO.; TASK NO. PP 013-08-01; WORK UNIT ACCESSION NO NR 056-68

11. TITLE (Include Security Classification) Utilization of a Highly Correlated Cluster Model for Interpretation of Electronic Spectroscopic Data for the High Temperature Superconductors. (Uncl.)

12. PERSONAL AUTHOR(S) D. E. Ramaker

13a. TYPE OF REPORT	13b. TIME COVERED	14. DATE OF REPORT (Year, Month, Day)	15. PAGE COUNT
Interim Technical	FROM _____ TO _____	December 1988	7

16. SUPPLEMENTARY NOTATION
Prepared for publication in AIP/AVS Topical Conference Proceedings

17. COSATI CODES		
FIELD	GROUP	SUB-GROUP

18. SUBJECT TERMS (Continue on reverse if necessary and identify by block number)
Superconductivity, Hubbard Model , Photoelectron Spectroscopy, Auger Spectroscopy, Copper Oxides (MAN)

19. ABSTRACT (Continue on reverse if necessary and identify by block number)

We have consistently interpreted electron spectroscopic data for the high temperature superconductors utilizing a highly-correlated CuO_n cluster model, and an extended Hubbard Hamiltonian which includes the inter-site Cu-O and O-O U_{pp} parameters. The data indicate much larger U_p and U_{pp} values than found in other typical highly conductive metals. Previously unassigned features in the data are now assigned within the model.

20. DISTRIBUTION / AVAILABILITY OF ABSTRACT	21. ABSTRACT SECURITY CLASSIFICATION
☒ UNCLASSIFIED/UNLIMITED ☒ SAME AS RPT. ☐ DTIC USERS	Unclassified
22a. NAME OF RESPONSIBLE INDIVIDUAL Dr. David L. Nelson	22b. TELEPHONE (Include Area Code) (202) 696-4410 / 22c. OFFICE SYMBOL

DD FORM 1473, 84 MAR — 83 APR edition may be used until exhausted. All other editions are obsolete.

SECURITY CLASSIFICATION OF THIS PAGE
Unclassified

(1)

UTILIZATION OF A HIGHLY-CORRELATED CuO_6 CLUSTER MODEL TO INTERPRET ELECTRON SPECTROSCOPIC DATA FOR THE HIGH-TEMPERATURE SUPERCONDUCTORS

David E. Ramaker[a]
Department of Chemistry, George Washington University
Washington, DC 20052, USA

ABSTRACT

We have consistently interpreted electron spectroscopic data for the high temperature superconductors utilizing a highly-correlated CuO_6 cluster model, and an extended Hubbard Hamiltonian which includes the inter-site Cu-O U_{pd} and O-O U_{pp} parameters. The data indicate much larger U_p and U_{pp} values than found in other typical highly conductive metals. Previously unassigned features in the data are now assigned within the model.

INTRODUCTION

In this work we summarize results of an interpretation of electron spectroscopic data for the high temperature superconductors. The data interpreted include the valence band (VB), Cu 2p, and O 1s photoelectron data (UPS and XPS), the Cu $L_{23}VV$, Cu $L_{23}M_{23}V$, and O KVV Auger data, and the O K and Cu L_{23} x-ray absorption and emission (XANES and XES) data. Published data for polycrystalline and single crystal samples of $La_{2-x}Ba_xCuO_4$ and $YBa_2Cu_3O_{7-x}$ (herein referred to as the La and 123 HTSC's) are considered along with that for CuO and Cu_2O.

The basic electronic structure of the HTSC's can be described with the Anderson Hamiltonian utilized by Sawatzky and coworkers[1,2]. It includes the transfer or hopping integral t, the Cu and O orbital energies ϵ_d and ϵ_p, the core polarization energy Q_d, and the intra-site Coulomb repulsion energies U_d and U_p (the latter sometimes are assumed to be zero). This model is most useful when the U's are large relative to the band widths[1], i.e. when correlation effects dominate hybridization effects. A $CuO_6^{(10-z)-}$ cluster model, which is also reasonably valid when U >> t, simplifies the model further[1]. We utilize an extended Hubbard model by adding the inter-site repulsion energies U_{dp} and U_{pp} (i.e. between neighboring Cu-O and O-O atoms). The addition of these interactions is important for understanding many of the features in the data.

RESULTS

Our results for the Hubbard parameters are summarized at the top of Table I. Other estimates of these Hubbard U and ϵ parameters have been reported previously for the HTSC's[2-4]. These were obtained empirically from the Cu 2p XPS and the VB UPS data utilizing the Anderson model. Our optimal extended Hubbard

[a]Supported in part by the Office of Naval Research.

results indicate that U_p = 12 and U_{pp}° = 4.5 eV for 123. These are much larger than previously thought for these metallic systems, although U_p-U_{pp}° is in agreement with the best theoretical results above.

An upper estimate of the two-center pp° hole-hole repulsion, U_{pp}°, can be obtained from the Klopman approximation[7],

$$U_{ij} = e^2/(r_{ij}^2 + (2e^2/(U_i + U_j))^2)^{1/2}, \quad (1)$$

where r_{ij} is the interatomic distance and U_i and U_j are the corresponding intra-atomic repulsion energies. Equation 1 gives a value for U_{pp}° around 4.8 eV assuming r_{o-o} is 2.7 A°. The experimental energies of 9.5 and 5.0 eV for the pp^o_b and pp^o_a features in 123 suggests that the pp° final state energy is 7.2 eV. This gives an empirical estimate for U_{pp}° of 4.2 eV, very close to the Klopman theoretical result, which does not include the effects of interatomic screening.

The above result shows that metallic screening of two holes, which are spatially separated on neighboring O atoms, is not very significant. This is in contrast to two Cu-O holes, where Table 1 indicates the optimal U_{dp} = 1 eV, while eq. 1 estimates U_{dp} at 6.1 eV assuming r_{c-o} is 1.9 A°. This large reduction in U_{dp} may result from charge transfer into the Cu 4sp levels to screen the Cu-O holes. Although metallic screening, which results from virtual electron-hole (e-p) pair excitations at the Fermi level, is not expected to be large in an insulator such as CuO, screening effects are expected to be much larger in metals, such as the HTSC's. The above results show that U_{dp} is significantly reduced in both, and U_{pp}° remains large in both. The lack of a significant change in the U's between CuO and the HTSC's indicates that the DOS at the Fermi level in the HTSC's must be very small.

Table 1 also correlates the calculated energies of the excited states with features in the experimental data. The $CuO_n^{(2n-2)-}$ cluster has one hole shared between the Cu 3d and O 2p shells in the ground state, which we term the v (valence) states. The spectroscopic final states reflect multi-hole states, e.g. v^2, cv (c = core) etc. The v states, as reflected by the theoretical DOS[8], have the Cu-O bonding ($\uparrow_b$) and antibonding ($\uparrow_a$) orbitals centered at 4 and 0 eV, respectively, and the nonbonding Cu and O orbitals at 2 eV. The O features each have a width 2Γ = 4 eV due to the O-O bonding and antibonding character and the Cu-O dispersion. We also define the Cu-O hybridization shift $\delta_1 = [(\Delta^2+4t^2)^{1/2} - \Delta]/2$, which is utilized in Table 1 to give the energies. Thus, the ground state of an average CuO_n cluster is located at 1 eV having the energy $\varepsilon_d - \delta_1 + \Gamma/2 = \varepsilon_d - \alpha$, which we use as a reference energy for the excited states. In CuO, the hybridization shift Γ is smaller, and we shall see below that $\Delta = \varepsilon_p - \varepsilon_d$ has increased to 1 eV.

Those clusters containing additional charge carrier holes (these exists in doped La, and 123 when x > 0.5) actually have two holes per CuO_n cluster. The average v^2 ground state, which is dominated by the pp^o configuration, i.e. the charge carrier holes spend most of their time on the O atoms, so we indicate this ground state by the

TABLE 1 Summary of hole states revealed in the spectroscopic data, and estimated energies using the following optimal values for the Hubbard parameters in eV[e]:

δ_1 = 2	ε_d = 2	U_p = 12, 13	U_d =9.5,10.2
δ_2 = 0.5,0.8	ε_p = 2, 3	U_{pp}[a] = 4.5, 4	U_{dp} =1
Γ = 2	U_{pp}[b] = 0.	U_{cp}[a] = 2	Q_d =9
α = 1, 0.5	β = 2	Δ = 0, 1.	K= 4

State[b]	Energy expression	Calc. E. eV[c,d]	Exp. E. eV[c]	Remark
	G.S. and IPES, v			
ψ_a) d	$\varepsilon_d - \delta_1 \mp \Gamma$	0 ∓ 2	-	heavily
ψ_b) p	$\varepsilon_p + \delta_1 \mp \Gamma$	4 ∓ 2	-	mixed
	UPS and XES, v^2			
1)[a] pp^b	$\varepsilon_p + \Delta - \delta_2 + \alpha$	2.5	2.5	heavily
2)[a] dp	$\varepsilon_p + U_{dp} + \delta_2 + \alpha$	4.5	4.2	mixed
3) pp^a	$\varepsilon_p + \Delta + U_{pp}$[a] $- \Gamma + \alpha$	5.5	5.	
4) pp^b	$\varepsilon_p + \Delta + U_{pp}$[a] $+ \Gamma + \alpha$	9.5	9.5	mystery peak
5) d^2	$\varepsilon_d + U_d + \alpha$	12.5	12.5	Cu sat.
6) p^2	$\varepsilon_p + \Delta + U_p + \alpha$	15	16	
	Cu 2p XPS, cv			
d → cp	$\varepsilon_c + \Delta + \alpha$	ε_c + 1	E_{1p}	main
cd	$\varepsilon_c + Q_d + \alpha$	ε_c + 10	E_{1p}+9.2	sat.
	Cu 2p XPS for $NaCuO_2$; $pp^b \rightarrow cv^2$			
$pp^b \rightarrow cpp^b$	$\varepsilon_c + \delta_2 + \beta$	ε_c + 2.5	ε_c+2.2	main
cpp^a	$\varepsilon_c + U_{pp}$[a] $- \Gamma + \delta_2 + \beta$	ε_c + 4.5	ε_c+5	?
cpp^b	$\varepsilon_c + U_{pp}$[a] $+ \Gamma + \delta_2 + \beta$	ε_c + 8.5	ε_c+9	?
cdp	$\varepsilon_c - \Delta + Q_d + U_{dp} + \delta_2 + \beta$	ε_c +11.5	ε_c+11	sat.
cp^2	$\varepsilon_c + U_p + \delta_2 + \beta$	ε_c +15.5	ε_c+14	sat.?
	O 1s XPS, cv			
d → cd	$\varepsilon_c + \alpha$	ε_c + 1	E_{1s}	main
cp^b	$\varepsilon_c + \Delta + \alpha$	ε_c + 1	E_{1s}	main
cp^a	$\varepsilon_c + \Delta + U_{cp}$[a] $+ \alpha$	ε_c + 3	E_{1s}+2 ?	tail
cp	$\varepsilon_c + \Delta + Q_p + \alpha$	?	?	not obs
$pp^b \rightarrow cdp^b$	$\varepsilon_c - \Delta + U_{dp} + \delta_2 + \beta$	ε_c+3.5	E_{1s}+2 ?	tail
	Cu L_3VV AES, v^2			
dpp^b	$2\varepsilon_p + 2U_{dp} + \alpha$	7	7	2 cent.
dpp^a	$2\varepsilon_p + U_{pp}$[a] $+ 2U_{dp} + \alpha$	11.5	-	no mix
d^2p	$\varepsilon_d + \varepsilon_p + U_d + 2U_{dp} - \delta_2 + \alpha$	16	15.5	main
dp^2	$2\varepsilon_p + U_p + 2U_{dp} + \delta_2 + \alpha$	19.5	18-25	sat.

TABLE 1 (cont.)

State[b]	Energy expression	Calc. E. eV[c,d]	Exp. E. eV[c]	Remark
	Cu $L_3M_{2,3}V$ AES, cv^2			
cdp	$\epsilon_c+\epsilon_p+Q_d+U_{dp}-K+\alpha$	ϵ_c +9	E_{2p}+10	main, ^1L
		ϵ_c+17	E_{2p}+18	main, ^3L
cp^2	$\epsilon_c+\epsilon_p+\Delta+U_p+\alpha$	ϵ_c+15	-	not
cd^2	$\epsilon_c+\epsilon_d+U_d+2Q_d+\alpha$	ϵ_c+30.5	-	obs.
	Cu $L_{2,3}$ EELS, c			
d → c	$\epsilon_c-\epsilon_d+\delta_1$	E_{2p}-1	E_{2p}-1.4	edge
cp<u>CB</u>	$\epsilon_c+\Delta-CB+\alpha$	E_{2p}-CB	E_{2p}+1.2	upper
pp^p → cp	$\epsilon_c-\epsilon_p+\delta_2+\beta$	E_{2p}-0.5	E_{2p}	middle
	O K EELS, c			
d → c	$\epsilon_c-\epsilon_d+\delta_1$	E_{1s}-1	E_{1s}	edge
cd<u>CB</u>	$\epsilon_c-CB+\alpha$	E_{2s}-CB	E_{1s}+1.7	upper
pp^p → cd	$\epsilon_c-\Delta-\epsilon_p+\delta_2+\beta$	E_{1s}-0.5	-	not obs

[a]Parameters for 123 indicated first, those for CuO second.
[b]The dominant character in the hybridized states is given.
[c]The Calc. E and Exp. E columns indicate the results for 123, except for the "Cu 2p XPS, $pp^p \rightarrow cv^2$" section, which is for $NaCuO_2$.
[d]The calculated E is defined relative to the ground v^1 (d) state energy = $\epsilon_d - \alpha$, or to the v^2 (pp^p) ground state energy = $2\epsilon_p-\delta_2-\beta$. The v^1(d) energy defines the Fermi level relative to the vacuum level at zero.
[e]The dominant character switches as described in the text, and thus the sign in front of δ_2 is the opposite for CuO.

parameters in Table 1 were obtained by considering this same data plus XANES, Auger and XES data. Although we are in general agreement with the reported magnitudes for most of the parameters, our U_d value is larger by about 2-3 eV so that it is consistent with the AES data. In Table 1, we indicate the location of two valence holes by d (Cu 3d) or p (O 2p). In the case of two holes on the oxygens, we distinguish two holes on the same O (p^2), on ortho neighboring O atoms (pp^o), or on para O atoms (pp^p) of the cluster. Furthermore, neighboring pp^o holes can dimerize[5], so we distinguish between two holes in bonded (pp^o_b) and antibonded (pp^o_a) O pairs.

The magnitudes of the U parameters are critical to the mechanism for the superconductivity. As a consequence, much effort has also gone into theoretically calculating these parameters, but wide disagreement still exists over the magnitudes. Theoretical values for U_d in the range 6.5-10 eV, U_p (actually $U_p-U_{pp}{}^o$) in the range 7-14 eV, and U_{dp} in the range 0.6-1.6 eV have been reported[6], with the smaller results favored based on the quality of the calculations. No results for $U_{pp}{}^o$ have been reported. Our empirical

notation pp^n. We use $2\varepsilon_p - \delta_z - \delta$ as the energy of the pp^n ground state relative to the vacuum level, where δ = 2 eV is the energy shift between the principal pp^n UPS final state at 2.5 eV and the lowest ground pp^n states around 0.5 eV from the Fermi level.

The correlation between the calculated energies and experimental features, utilizing the indicated optimal Hubbard parameters is very good. Details of this work are published elsewhere[9]. Figs. 1 and 2 show examples of the UPS and Cu AES data for 123 and CuO_2, which reveal some of the features itemized in Table 1; the remaining data are published elsewhere.

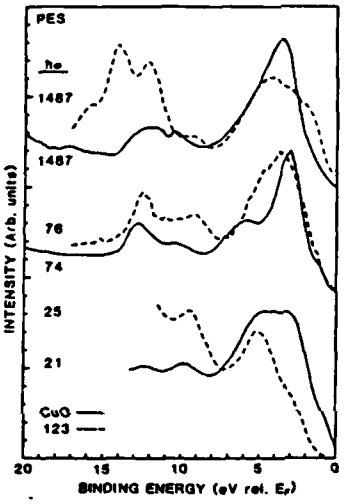

Figure 1. Comparison of UPS spectra for CuO and 123 taken with the indicated photon energies in eV. Data for CuO from refs. 10 (hν = 1487), 11 (hν = 74) and 12 (hν = 21). Data for 123 from ref. 13 (hν = 25 and 74) and 14 (hν = 1487).

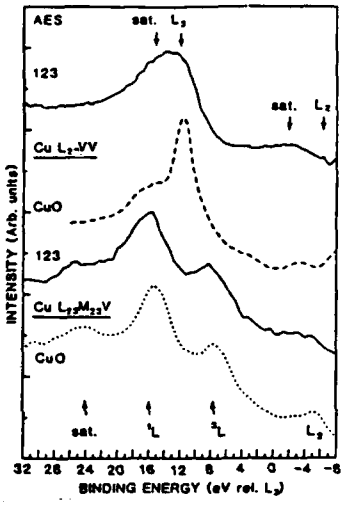

Figure 2. Comparison of Auger data for the materials indicated. $L_{23}VV$ data for CuO and 123 from ref. 15. $L_{23}M_{23}V$ data for CuO from ref. 16 and for 123 from Ref. 9. The $L_{23}VV$ data is on a 2-hole binding energy scale = $E_{L3}-E_{L2}$, and the $L_{23}M_{23}V$ on a 1-hole scale = $E_{L3}-E_{L2}-E_{N3}$, where E_{L3} = 933.4 and E_{N3} = 77.3 eV[11,12].

SUMMARY AND CONCLUSIONS

This work has allowed us to assign some previously unassigned features in the data, and greatly increased our understanding of the

dynamical electronic processes which produce these features. We itemize our conclusions as follows:

1) A switch in the character of state 1 (see Table 1) from more dp to pp^n and vice versa for state 2 between CuO and 123 arises because Δ decreases from 1 eV to 0 eV. The smaller Δ in 123, due to a smaller ϵ_p polarization energy, is consistent with the Cu 2p XPS and XES data (the latter showing this effect dramatically)[17,18]. Since state 1 is more of pp^n character in the SC's, the "charge carrier holes" (present in the La after Sr doping and in the 123 when 7-x is greater than 6.5) spend more time on the oxygens in 123 than in CuO.

2) The pp^n state is believed to be responsible for the "mystery" peak found at 9.5 eV in the UPS. Figure 1 indicates that such a feature also appears for CuO[11,12]. This feature does not appear for Cu_2O, as expected since UPS reflects the one-hole DOS in Cu_2O. Thus this feature is not unique to the SC's; it naturally appears for those systems with two-hole photoemission final states.

3) Although Cu_2O, CuO, and $NaCuO_2$ have a formal Cu valence of +1, +2, and +3, in the current picture they reflect the cv^n DOS, with n=0, 1, and 2. Furthermore, we consistently predict the "chemical shifts" in the primary Cu 2p XPS peaks. Whereas, Cu_2O exhibits just a primary core hole c state at energy ϵ_c, CuO has its primary cd feature energy shifted by $\Delta+\alpha$ relative to ϵ_c, and the primary cpp^n feature for $NaCuO_2$ by $\delta_2+\delta$ (Table 1), which is consistent with the experimental data[17]. The width of the primary feature is seen to correlate with the intensity of the satellite, and is not due to the O p band width as suggested by others[18].

4) The increased "satellite" feature at 19 eV in the Cu $L_{23}VV$ Auger line shape for the HTSC's compared with CuO[15,16] (see Fig. 2) arises because of increased final-state configuration mixing between the d^2p and dp^2 states. Its intensity is increased in 123 relative to CuO because the energy separation (before hybridization) between d^2p and dp^2 has decreased from 3.8 eV in CuO to 2.5 eV in 123. We have indicated this mixing in Table 1 by adding the hybridization shifts δ_2 to the energy expressions for these two states.

5) We find that the initial-core shakeup (ICSU) process, which is known to be responsible for the satellite features in the Cu 2p XPS data[1], does not produce satellites in the AES or XES data, because the ICSU states generally "relax" to the primary states of the same symmetry before the core level decay. Such a relaxation is expected when the ICSU excitation energy is larger than the core level width[19]. Previously, vanderLaan et al.[1], for the Cu halides, suggested that the intensity of these ICSU states in the XPS should be quantitatively reflected in the intensity of the Auger satellites found in the $L_{23}VV$ lineshapes. The data do not indicate this however. We previously[15] indicated that a fraction of these ICSU states probably resulted in Auger satellites for the HTSC's, and that this fraction becomes larger as the the covalency of the HTSC material increases. This work indicates rather that the ICSU states relax before the core level decay to states of the same symmetry, provided they have a ICSU excitation energy that is much greater

than the core level width. We believe this to be a general result, at least in the Cu^{+2} materials.

6) The EELS and XANES data[20,21] reflect the contributions from three possible transitions; the dominant d → c contribution nearest the Fermi level, the $pp^n \rightarrow cv$ (v = d or p) contribution resulting from the carrier hole states, as well as the cv<u>CB</u> contribution well above the Fermi level[22]. Here <u>CB</u> represents an electron present in the higher Cu 4sp or O 3p "conduction band". The latter two contributions are not always resolved, and sometimes have been confused in the literature[20-22].

7) All of the temperature effects seen in the spectroscopic data[23-26] can be attributed to a single phenomenon, namely a decrease in c_p due to increased metallic screening, or long range polarization. This is consistent with the decrease in the primary cp peak energy in the Cu 2p XPS, while the cd satellite remains unshifted. The larger energy separation between the cd and cp states decreases the mixing which causes the satellite to decrease in intensity and the main peak to get narrower. Although the primary cd peak does not shift in the O 1s XPS, a slight shift to lower energy is seen in the cp^n and cp^e contributions at lower temperature, as expected with a decrease in c_p. The UPS spectra show a skewing toward the Fermi level at lower temperature, as expected with a decrease in c_p. Finally the growth of the satellite intensity in the Cu $L_{23}VV$ Auger lineshape is consistent with a decrease in e_p. The increased metallic like screening or polarization which appears to occur at lower temperature, reducing c_p, probably involves the grain boundaries, since the more recent data for the single crystal samples do not change with temperature[27].

In summary, an interpretation of the data utilizing a highly correlated CuO_8 cluster model shows that a single set of Hubbard parameters predicts all of the state energies. Changes in the data between CuO and the HTSC's arises primarily from a reduction in c_p; this reduction continues with decreasing temperature in the HTSC's due to increased metallic screening. Compared with CuO, the HTSC's show an increased covalent interaction between the Cu-O bonds. The large size of U_{pp}^e, and the temperature dependence, reveal that metallic screening is incomplete, and hence that the DOS at the Fermi level in the HTSC's is relatively small.

REFERENCES

1. G. vanderLaan et al., Phys. Rev. 24, 4369 (1981); G.A. Sawatzky et al., Phys. Rev. Lett. 53, 2339 (1985); J. Zaanen et al., Phys. Rev. B33, 8060 (1986).
2. Z. Shen et al., Phys. Rev. B36, 8414 (1987).
3. A. Fujimori et al., Phys. Rev. B35, 8814 (1987).
4. J.C. Fuggle et al., Phys. Rev. B37, 1123 (1988).
5. R.A. de Groot, H. Gutfreund, and M. Weger, Sol. State Commun. 63, 451 (1987); W. Folkerts et al., J. Phys. C: Solid State Phys. 20, 4135 (1987); A. Manthiram, X.X. Tang, and J.B. Goodenough, Phys. Rev. B37, 3734 (1988).

6. C.P. Chen et al., unpublished; A.K. McMahan, R.M. Martin, and S. Satpathy, unpublished; M. Schluter, M.S. Hybertsen, and N. E. Christensen, Proc. Intn. Conf. High T_c Superconductors and Materials and Mechanisms of Superconductivity, J. Muller and J.L. Olsen, Eds., (Interlaken, Switzerland, 1988).
7. G. Klopman, J. Am. Chem. Soc. 86, 4550 (1964).
8. J. Redinger et al., Phys. Lett. 124, 463 and 469 (1987).
9. D.E. Ramaker, N.H. Turner, and F.L. Hutson, submitted.
10. A. Rosencwaig and G.K. Wertheim, J. Elect. Spectrosc. Related Phenom. 1, 493 (1972/73).
11. M.R. Thuler, R.L. Benbow, and Z. Hurych, Phys. Rev. B26, 669 (1982).
12. C. Benndorf et al., J. Electron. Spectrosc. Related Phenom. 19, 77 (1980).
13. N.G. Stoffel et al., Phys. Rev. B37, 7952 (1988); B38, July (1988).
14. D.C. Miller et al., in Thin Film Processing and Characterization of High Temperature Superconductors, J.M. Harper, J.H. Colton, and L.C. Feldman, Eds., AVS Series No. 3 (AIP: New York, 1988) p 336.
15. D.E. Ramaker et al., Phys. Rev. 36, 5672 (1987).
16. P.E. Larson, J. Electron Spectrosc. Related Phenom. 4, 213 (1974).
17. P. Steiner et al., Z. Phys. B- Condensed Matter 67, 497 (1987).
18. D.D. Sarma, Phys. Rev. B37, 7948 (1988).
19. J.W. Gadzuk and M. Sunjic, Phys. Rev. B12, 524 (1975).
20. D.D. Sarma et al., Phys. Rev. B37, 9784 (1988).
21. N. Nucker et al., Z. Phys. B: Cond. Matter 67, 9 (1987); Phys. Rev. 37, 5158 (1988).
22. A. Bianconi et al., Solid State Commun. 63, 1009 (1987); Intn. J. Modern Phys. 131, 853 (1987).
23. N.S. Kohiki and T. Hamada, Phys. Rev. B36, 2290 (1987).
24. B. Dauth et al., Z. Phys. B- Condensed Matter 68, 407 (1987).
25. D.H. Kim et al., Phys. Rev. B37, 9745 (1988).
26. A. Balzarotti et al., Phys. Rev. B36, 8285 (1987).
27. J. Weaver and P. Steiner, private communication.

TECHNICAL REPORT DISTRIBUTION LIST, GEN

	No. Copies
Office of Naval Research Attn: Code 1113 800 N. Quincy Street Arlington, Virginia 22217-5000	2
Dr. Bernard Douda Naval Weapons Support Center Code 50C Crane, Indiana 47522-5050	1
Naval Civil Engineering Laboratory Attn: Dr. R. W. Drisko, Code L52 Port Hueneme, California 93401	1
Defense Technical Information Center Building 5, Cameron Station Alexandria, Virginia 22314	12 high quality
DTNSRDC Attn: Dr. H. Singerman Applied Chemistry Division Annapolis, Maryland 21401	1
Dr. William Tolles Superintendent Chemistry Division, Code 6100 Naval Research Laboratory Washington, D.C. 20375-5000	1
Dr. David Young Code 334 NORDA NSTL, Mississippi 39529	1
Naval Weapons Center Attn: Dr. Ron Atkins Chemistry Division China Lake, California 93555	1
Scientific Advisor Commandant of the Marine Corps Code RD-1 Washington, D.C. 20380	1
U.S. Army Research Office Attn: CRD-AA-IP P.O. Box 12211 Research Triangle Park, NC 27709	1
Mr. John Boyle Materials Branch Naval Ship Engineering Center Philadelphia, Pennsylvania 19112	1
Naval Ocean Systems Center Attn: Dr. S. Yamamoto Marine Sciences Division San Diego, California 91232	1

ABSTRACTS DISTRIBUTION LIST, 056/625/629

Dr. F. Carter
Code 6170
Naval Research Laboratory
Washington, D.C. 20375-5000

Dr. Richard Colton
Code 6170
Naval Research Laboratory
Washington, D.C. 20375-5000

Dr. Dan Pierce
National Bureau of Standards
Optical Physics Division
Washington, D.C. 20234

Dr. R. G. Wallis
Department of Physics
University of California
Irvine, California 92664

Dr. D. Ramaker
Chemistry Department
George Washington University
Washington, D.C. 20052

Dr. J. C. Hemminger
Chemistry Department
University of California
Irvine, California 92717

Dr. T. F. George
Chemistry Department
University of Rochester
Rochester, New York 14627

Dr. G. Rubloff
IBM
Thomas J. Watson Research Center
P.O. Box 218
Yorktown Heights, New York 10598

Dr. J. Baldeschwieler
Department of Chemistry and
Chemical Engineering
California Institute of Technology
Pasadena, California 91125

Dr. Galen D. Stucky
Chemistry Department
University of California
Santa Barbara, CA 93106

Dr. A. Steckl
Department of Electrical and
Systems Engineering
Rensselaer Polytechnic Institute
Troy, New York 12181

Dr. John T. Yates
Department of Chemistry
University of Pittsburgh
Pittsburgh, Pennsylvania 15260

Dr. R. Stanley Williams
Department of Chemistry
University of California
Los Angeles, California 90024

Dr. R. P. Messmer
Materials Characterization Lab.
General Electric Company
Schenectady, New York 22217

Dr. J. T. Keiser
Department of Chemistry
University of Richmond
Richmond, Virginia 23173

Dr. R. W. Plummer
Department of Physics
University of Pennsylvania
Philadelphia, Pennsylvania 19104

Dr. E. Yeager
Department of Chemistry
Case Western Reserve University
Cleveland, Ohio 41106

Dr. N. Winograd
Department of Chemistry
Pennsylvania State University
University Park, Pennsylvania 16802

Dr. Roald Hoffmann
Department of Chemistry
Cornell University
Ithaca, New York 14853

Dr. Robert L. Whetten
Department of Chemistry
University of California
Los Angeles, CA 90024

Dr. Daniel M. Neumark
Department of Chemistry
University of California
Berkeley, CA 94720

Dr. G. H. Morrison
Department of Chemistry
Cornell University
Ithaca, New York 14853

//

ABSTRACTS DISTRIBUTION LIST, 056/625/629

Dr. J. E. Jensen
Hughes Research Laboratory
3011 Malibu Canyon Road
Malibu, California 90265

Dr. J. H. Weaver
Department of Chemical Engineering
and Materials Science
University of Minnesota
Minneapolis, Minnesota 55455

Dr. A. Reisman
Microelectronics Center of North Carolina
Research Triangle Park, North Carolina
27709

Dr. M. Grunze
Laboratory for Surface Science
and Technology
University of Maine
Orono, Maine 04469

Dr. J. Butler
Naval Research Laboratory
Code 6115
Washington D.C. 20375-5000

Dr. L. Interante
Chemistry Department
Rensselaer Polytechnic Institute
Troy, New York 12181

Dr. Irvin Heard
Chemistry and Physics Department
Lincoln University
Lincoln University, Pennsylvania 19352

Dr. K. J. Klaubunde
Department of Chemistry
Kansas State University
Manhattan, Kansas 66506

Dr. C. B. Harris
Department of Chemistry
University of California
Berkeley, California 94720

Dr. R. Bruce King
Department of Chemistry
University of Georgia
Athens, Georgia 30602

Dr. R. Reeves
Chemistry Department
Renssaeler Polytechnic Institute
Troy, New York 12181

Dr. Steven M. George
Stanford University
Department of Chemistry
Stanford, CA 94305

Dr. Mark Johnson
Yale University
Department of Chemistry
New Haven, CT 06511-8118

Dr. W. Knauer
Hughes Research Laboratory
3011 Malibu Canyon Road
Malibu, California 90265

Dr. Theodore E. Madey
Surface Chemistry Section
Department of Commerce
National Bureau of Standards
Washington, D.C. 20234

Dr. J. E. Demuth
IBM Corporation
Thomas J. Watson Research Center
P.O. Box 218
Yorktown Heights, New York 10598

Dr. M. G. Lagally
Department of Metallurgical
and Mining Engineering
University of Wisconsin
Madison, Wisconsin 53706

Dr. R. P. Van Duyne
Chemistry Department
Northwestern University
Evanston, Illinois 60637

Dr. J. M. White
Department of Chemistry
University of Texas
Austin, Texas 78712

Dr. Richard J. Saykally
Department of Chemistry
University of California
Berkeley, California 94720

ABSTRACTS DISTRIBUTION LIST, 056/625/629

Dr. G. A. Somorjai
Department of Chemistry
University of California
Berkeley, California 94720

Dr. J. Murday
Naval Research Laboratory
Code 6170
Washington, D.C. 20375-5000

Dr. W. T. Peria
Electrical Engineering Department
University of Minnesota
Minneapolis, Minnesota 55455

Dr. Keith H. Johnson
Department of Metallurgy and
Materials Science
Massachusetts Institute of Technology
Cambridge, Massachusetts 02139

Dr. S. Sibener
Department of Chemistry
James Franck Institute
5640 Ellis Avenue
Chicago, Illinois 60637

Dr. Arold Green
Quantum Surface Dynamics Branch
Code 3817
Naval Weapons Center
China Lake, California 93555

Dr. A. Wold
Department of Chemistry
Brown University
Providence, Rhode Island 02912

Dr. S. L. Bernasek
Department of Chemistry
Princeton University
Princeton, New Jersey 08544

Dr. W. Kohn
Department of Physics
University of California, San Diego
La Jolla, California 92037

Dr. Stephen D. Kevan
Physics Department
University Of Oregan
Eugene, Oregon 97403

Dr. David M. Walba
Department of Chemistry
University of Colorado
Boulder, CO 80309-0215

Dr. L. Kesmodel
Department of Physics
Indiana University
Bloomington, Indiana 47403

Dr. K. C. Janda
University of Pittsburg
Chemistry Building
Pittsburg, PA 15260

Dr. E. A. Irene
Department of Chemistry
University of North Carolina
Chapel Hill, North Carolina 27514

Dr. Adam Heller
Bell Laboratories
Murray Hill, New Jersey 07974

Dr. Martin Fleischmann
Department of Chemistry
University of Southampton
Southampton SO9 5NH
UNITED KINGDOM

Dr. H. Tachikawa
Chemistry Department
Jackson State University
Jackson, Mississippi 39217

Dr. John W. Wilkins
Cornell University
Laboratory of Atomic and
Solid State Physics
Ithaca, New York 14853

Dr. Ronald Lee
R301
Naval Surface Weapons Center
White Oak
Silver Spring, Maryland 20910

Dr. Robert Gomer
Department of Chemistry
James Franck Institute
5640 Ellis Avenue
Chicago, Illinois 60637

Dr. Horia Metiu
Chemistry Department
University of California
Santa Barbara, California 93106

Dr. W. Goddard
Department of Chemistry and Chemical
Engineering
California Institute of Technology
Pasadena, California 91125